Superrotation in an Axisymmetric Shallow Water Model of the Upper Troposphere

Karen M. Shell

1 Introduction

Superrotation is defined by zonal mean zonal winds that have a greater angular momentum than the surface of the earth at the equator. In order for the circulation to be inertially stable, the angular momentum of the zonal winds must decrease poleward. Thus, if the winds at the equator are not superrotating, the winds are nowhere superrotating.

On the earth, the equatorial tropospheric winds are slightly easterly, so they have less angular momentum than the earth's surface at the equator. Thus, the earth's troposphere is not superrotating. However, superrotation occurs during the westerly phase of the Quasi-Biennial Oscillation (QBO) in the stratosphere, as well as on other planets, such as Jupiter and Saturn, and on our sun. These cases raise the question of whether the earth's troposphere could be superrotating under earth-like conditions.

Superrotation has appeared in simple models of the earth's atmosphere. Suarez and Duffy [1] obtained superrotating states in a two-layer model when they applied a zonally asymmetric tropical heating. For certain strengths of the forcing, they found multiple equilibria. Once superrotation was established in the model, the system would remain superrotating if they removed the asymmetric heating. Saravanan [2] used a two-layer model as well but applied a torque rather than asymmetric heating to produce superrotation. Recently, Huang et al [3] found slight superrotation in a coupled GCM climate change simulation with tripled $C0_2$. This experiment suggests the possibility that superrotation could develop due to anthropogenic climate change, though much more work is needed to determine if this is a realistic possibility. Held summarizes the research on superrotation in earth-like atmospheric models [4].

Suarez and Duffy and Saravanan attributed the bifurcations they obtained to a feedback between the forcing (whether generated by asymmetric heating or an applied torque) and the eddies. The forcing accelerates equatorial winds, and the eddies tend to decelerate equatorial winds. However, the effectiveness of the eddies decreases as the wind speed increases. Thus, increasing the forcing leads to stronger equatorial winds and thus less deceleration by the eddies, resulting in a positive feedback.

We looked for a similar bifurcation in an axisymmetric shallow water model of the upper troposphere. The model includes a torque that is directly applied to the equatorial region. In addition, the transport of mass (and thus momentum) from a non-moving lower layer can decelerate the flow around the equator. This deceleration depends on the wind speed at the equator, which depends on the strength of the forcing. We are interested in whether this feedback allows multiple equilibria for some ranges of the forcing. Since u is always superrotating with the applied force, we looked for multiple steady superrotating states, one weakly superrotating and one strongly superrotating, for the same set of parameters.

We attempted to add a parameterization of breaking Rossby waves to the model in order to see how waves affect the circulation. However, we were not successful because we could not get final states independent of the grid spacing.

Section 2 describes the shallow water model we used. In Section 3, we examine a simple analytical approximation to the full model to better understand the system. Section 4 describes the results of the numerical simulations. Our attempt to add breaking Rossby waves is discussed in Section 5. Finally, we present conclusions from this project in Section 6.

2 The Model

We modeled the troposphere using an axisymmetric (no variation in the longitudinal direction) one-and-a-half layer isentropic model on a sphere. The lower layer does not move, but it can exchange mass with the upper layer, thus affecting the height and zonal velocity of the upper layer. The upper portion of the troposphere is modeled using the shallow water equations for a spherical isentropic layer. The model determines the zonal velocity, u, meridional velocity, v, and height of the upper layer, h, as a function of time, t, and latitude, ϕ :

$$\frac{\partial u}{\partial t} + \frac{v}{a} \frac{\partial u}{\partial \phi} - 2\Omega v \sin \phi - \frac{uv \tan \phi}{a} = F + R - ku \tag{1}$$

$$\frac{\partial v}{\partial t} + \frac{v}{a}\frac{\partial v}{\partial \phi} + 2\Omega u\sin\phi + \frac{u^2\tan\phi}{a} = -\frac{g^*}{a}\frac{\partial h}{\partial \phi} - kv \tag{2}$$

$$\frac{\partial h}{\partial t} + \frac{1}{a\cos\phi} \frac{\partial hv\cos\phi}{\partial\phi} = -\frac{h - h_{eq}}{\tau},\tag{3}$$

where F is an applied forcing. The system is relaxed to a radiative equilibrium height, $h_{eq}(\phi)$, and

$$R = \begin{cases} \frac{h - h_{eq}}{\tau} \frac{u}{h} & (h - h_{eq} < 0)\\ 0 & (h - h_{eq} > 0) \end{cases}$$
(4)

is the deceleration of the zonal momentum due to mass moving from the lower layer to the upper layer as part of this height relaxation. Ω is the rotation rate, a is the radius of the earth, k is the frictional parameter, g^* is the reduced gravity, and τ is the relaxation time. All values are in MKS units.

The forcing F for the system is an applied torque centered around the equator and constant in time. Two types of forcing are used. (Figure 1 illustrates some of the forcing distributions.)

1. The first torque represents a flux of momentum from the lower layer:

$$F_1 = F_0 \cos^n \phi,$$

where F_0 is the forcing at the equator.

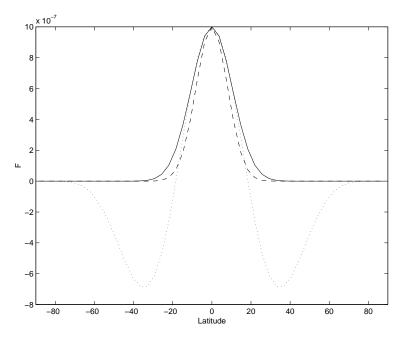


Figure 1: Example forcing distributions for $F_0 = 10^{-6}$. The solid line corresponds to the default forcing distribution $(F_1, n = 30)$. The dashed line corresponds to a narrower forcing $(F_1, n = 50)$. The dotted line corresponds to an angular momentum conserving forcing $(F_2, n = 9)$. For a given value of F_0 , the forcing distributions all have the same value at the equator.

2. The second torque represents a redistribution of angular momentum within the layer:

$$F_2 = F_0 \frac{h_0}{h} (-n \cos^{n-3} \phi + (n+1) \cos^{n-1} \phi),$$

where h_0 is the height of the layer at the equator. This forcing accelerates winds in the tropics and decelerates them in the midlatitudes, corresponding to waves excited in the tropics and breaking in the midlatitudes.

The height of the upper layer is relaxed back to the "radiative equilibrium" height, h_{eq} , which simulates the effects of radiation on the system. When radiation warms a portion of air in the lower layer, its potential temperature increases, and it moves to the upper layer, increasing the height of the upper layer. When the upper layer cools, some air moves down into the lower layer, decreasing the height of the upper layer. The radiative equilibrium is assumed to be in geostrophic balance with the "radiative equilibrium" wind:

$$u_{eq} = u_{0eq} \cos \phi,$$

where u_{0eq} is the radiative equilibrium wind at the equator. By integrating the geostrophic terms in equation (2):

$$2\Omega\sin\phi u_{eq} = -\frac{g^*}{a}\frac{\partial h_{eq}}{\partial\phi},$$

we obtain the equation for h_{eq} :

$$h_{eq} = h_{0eq} - \frac{a\Omega u_{0eq}}{g^*} \sin^2 \phi, \qquad (5)$$

where h_{0eq} is the radiative equilibrium height at the equator.

The relaxation back to the equilibrium height also affects the zonal momentum budget through term R in equation (1). Air that is brought up from the lower layer carries with it the momentum from the lower layer. Since the momentum of the lower layer is less that that of the upper layer, this process decreases the zonal momentum in the upper layer. However, air that moves from the upper layer down to the lower layer carries with it the momentum of the upper layer and thus does not affect the momentum in the upper layer. Presumably surface friction returns the velocity in the lower layer to zero. Note that the relaxation mass flux also should affect the meridional velocity. However, we have omitted this effect from equation (2) because v is very close to geostrophic balance.

To derive the effect of height relaxation on the zonal velocity, start by changing h based on the amount of mass added to the layer:

$$\frac{\partial h}{\partial t} = -\frac{h - h_{eq}}{\tau}.$$
(6)

The total angular momentum in the upper layer, hM, changes by the amount of mass added times the absolute angular momentum of the moving mass, M_r :

$$\frac{\partial(hM)}{\partial t} = -\frac{h - h_{eq}}{\tau}M_r$$

Using the chain rule and substituting in equation (6) yields

$$\frac{\partial M}{\partial t} = -\frac{(h - h_{eq})}{\tau} \frac{(M_r - M)}{h}$$

Since

$$M = (\Omega a \cos \phi + u) a \cos \phi,$$

we obtain an expression for the change to the zonal velocity:

$$\frac{\partial u}{\partial t} = -\frac{(h-h_{eq})}{\tau} \frac{(u_r-u)}{h}.$$

When $h - h_{eq}$ is positive, $u_r = u$ because the mass that moves has the same velocity as the layer. When, $h - h_{eq}$ is negative, u_r is the zonal velocity of the lower layer. Since the lower layer is not moving, we obtain equation (4). This term is the key term in our model, because it provides the positive feedback to the forcing. At equator, the forcing must balance the height relaxation term and friction. Since friction increases as the forcing (and thus the wind speed) increases, the height relaxation term is the required term for a bifurcation in this system.

2.1 Numerical Scheme

The model is solved numerically using a centered in space, leapfrog in time scheme with a Robert (asselin) filter to prevent the even and odd time time steps from drifting apart. The filter is applied to u, v, and h after the value at time t + 1 is calculated and has the following form:

$$X_{new}^{t} = (1 - 2\alpha)X_{old}^{t} + \alpha(X^{t-1} + X^{t+1})$$

The value of α does not affect the results, since we are interested in finding steady states. Note, however, that the choice of α might affect periodic solutions.

The value of the time step, Δt , does not affect the solution; however, if it is too high, the solution becomes unstable. Generally, I used values between 250 and 500 seconds.

The grid is staggered, with u and h gridpoints halfway between the v grid points. The staggered grid point method allows for easier calculation of gravity waves. The poles correspond to v grid points, and v is set to 0 here. The equator corresponds to a u and hgrid point.

The advective and Coriolis terms of Equation 1 are actually calculated in flux form as

$$\frac{\partial u}{\partial t} = \frac{1}{a\cos\phi} \frac{\partial M}{\partial t},$$

where M is the total angular momentum and is calculated so that

$$\frac{\partial(Mh)}{\partial t} = h\frac{\partial M}{\partial t} + M\frac{\partial h}{\partial t}.$$

2.2 Model without forcing

Figure 2 shows the steady state of the model with no forcing. For this run, we used values of $a = 6.37 \times 10^6$ m, $\Omega = 7.292 \times 10^{-5}$ rad/s, $g^* = 9.81 \times 0.1$ ms⁻², $\tau = 900000$ s, $k = 5 \times 10^{-9}$ s⁻¹, $h_{0eq} = 56632$ m, $u_{0eq} = 100$ m/s, and $\alpha = 0.5$. The number of v grid points is 200. Except for the grid spacing, which is normally 50 v grid points, these are the default values for all runs.

While the model uses similar parameters to those of the earth, it is not entirely earthlike. First, the atmosphere is not well-represented as two isentropic layers. The difference in potential temperature between the equator and the poles is about the same as the difference between the surface and the tropopause. Thus, the real atmosphere does not have an isentrope which divides the tropopapere into an upper and lower layer.

The height of the layer is too large because the radiative equilibrium u, u_{eq} is too large in the high latitudes. (Perhaps a different function for u_{eq} should be used, but the cosine function allows us to use a simple analytical model of the more complex computer model.) Since h is so large, the Hadley circulation is very weak, so the meridional velocity is smaller than it should be.

3 Analytical Calculations

In order to study the system more closely, we used a simple analytical model which approximates the full system of equations. The analytical model seeks to describe the state

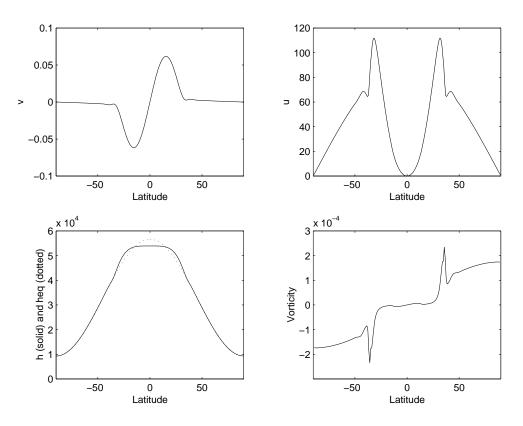


Figure 2: Steady state of the model with no forcing.

of the system using only u and h at the equator. By requiring that u and h are in steady state at the equator, we can determine which of these states is an equilibrium solution for a given set of parameters. This information gives us an idea of where to look for multiple equilibria.

The relation of the circulation to u and h at the equator can be explored using a simple Hadley cell model similar to the one used in Held and Hou [5]. The domain is divided into two regions. Close to the equator, the solution for h conserves angular momentum, while towards the poles, the solution is just the "radiative equilibrium" solution, h_{eq} . By matching these two solutions, we can determine the critical latitude, θ_c , which separates them.

Equation (5) describes the radiative equilibrium solution. To determine the angular momentum conserving solution, h_m , assume the height is in geostrophic balance with the angular momentum conserving wind:

$$u_m = \frac{u_0 + \Omega a \sin^2 \phi}{\cos \phi},\tag{7}$$

where u_0 is the zonal velocity at the equator. Integrating the geostrophic terms in equation (2) using the small angle approximation and the fact that $u_0 \ll \Omega a$,

$$h_m = h_0 - \frac{2a\Omega}{g^*} \left[u_0 \frac{\phi^2}{2} + \Omega a \frac{\phi^4}{4} \right],$$
(8)

where h_0 is the height of the layer at the equator.

Continuity of h at ϕ_c requires

$$h_{eq}(\phi_c) = h_m(\phi_c),\tag{9}$$

while mass conservation requires

$$\int_{0}^{\phi_c} h_{eq} \cos \phi d\phi = \int_{0}^{\phi_c} h_m \cos \phi d\phi.$$
(10)

Solving equations (9) and (10) assuming $u_0 \ll \Omega a$, $h_{0eq} \approx h_0$, and ϕ_c small yields equations for the critical latitude and the height at the equator in terms of u_0 :

$$\phi_c^2 = \frac{5}{3} \frac{u_{0eq} - u_0}{\Omega a}$$

$$h_0 - h_{0eq} = -\frac{5}{18g^*} (u_{0eq} - u_0)^2.$$
 (11)

Note that to get a real value for ϕ_c , u_0 must be less than u_{0eq} . When these computations are performed without the approximations for the parameter range we use, the results agree fairly well with this equation (Moehlis, personal communication), so we feel that the approximations are valid.

In order for u_0 and h_0 to be in steady state, the applied torque at the equator must balance the friction and the momentum exchange due to relaxation of the height to equilibrium:

$$F = \frac{h_{0eq} - h_0}{\tau} \frac{u_0}{h_0} + ku_0 \quad (h_0 < h_{0eq}).$$
(12)

Assuming the system is not far from radiative equilibrium, we approximate the height in the denominator as a constant, h_{0eq} . (Retaining the variation of height in the denominator does not greatly alter the solution and makes computation more difficult.)

Nondimensionalizing by

$$h_0 = Hh_{0eq}, \ u_0 = Uu_{0eq},$$

equations (11) and (12) become:

$$1 - H = p(U - 1)^2 \tag{13}$$

$$1 - H = \frac{q}{U} - r \tag{14}$$

where

$$q = \frac{F\tau}{u_{0eq}}, \ p = \frac{5}{18} \frac{u_{0eq}^2}{g^* h_{0eq}}, \ r = k\tau,$$

with q, p, and r all positive.

We are looking for solutions of these two equations for which U < 1 and 0 < H < 1, since our analytical model requires that $u_0 < u_{0eq}$ and $0 < h_0 < h_{0eq}$. Equilibrium solutions are solutions of the cubic equation

$$U^{3} - 2U^{2} + U\left(1 + \frac{r}{p}\right) - \frac{q}{p} = 0$$
(15)

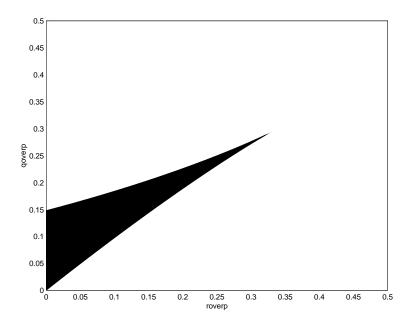


Figure 3: Region of multiple equilibria in analytical model. The dark region indicates values of $\frac{r}{p}$ and $\frac{q}{p}$ for which there exist multiple equilibria. q corresponds to the strength of the applied forcing; r corresponds to the friction; and p relates to the Hadley circulation.

There are three real solutions when

$$\left(-\frac{1}{9} + \frac{1}{3}\frac{r}{p}\right)^3 + \left(-\frac{1}{27} - \frac{1}{3}\frac{r}{p} + \frac{1}{2}\frac{q}{p}\right) < 0 \tag{16}$$

Otherwise, there is only one real solution, and we do not expect multiple equilibria in our model.

Figure 3 shows the parameter region where the simple model predicts multiple equilibria. In this region, the solution corresponding to the smallest u is stable while the middle solution is unstable. Thus, model runs that start with initial conditions between the lowest and the middle solutions will equilibrate to the lower superrotating state. When the third solution (highest u) is a valid solution, we expect the system to go to this state if the initial conditions are above the middle solution. However, the solution with the highest u is generally not valid because $u > u_{0eq}$; in these cases, we expect that systems with initial conditions above the middle solution will equilibrate to a higher u steady state, for which we do not have a model. The stability of the different equilibria can be verified using a potential function (Moehlis, personal communication).

We further examined the feedback in this simplified model. As the forcing increases, u increases, which in turn decreases the Hadley circulation. Thus, less mass is brought up from below to decelerate the upper layer. This deceleration, 1 - H, can be thought of as a "damping", r_h , caused by the relaxation of the height to the equilibrium height. Rearranging equation (14), we obtain an expression for U:

$$U = \frac{q}{r_h(U(q)) + r}.$$

We want to know how U changes with the forcing (q):

$$\frac{\partial U}{\partial q} = \left(\frac{1}{r_h + r}\right) \frac{1}{1 + \frac{q}{(r_h + r)^2} \frac{\partial r_h}{\partial U}}.$$

Using equation (13), which represents the Hadley circulation,

$$\frac{\partial U}{\partial q} = \left(\frac{1}{p(U-1)^2 + r}\right) \frac{1}{1 + \frac{2U(U-1)}{(U-1)^2 + r/p}}$$

When $\frac{\partial U}{\partial q}$ goes to infinity, U must jump to a different solution. This quantity goes to infinity when

$$U = \frac{2 \pm \sqrt{1 - \frac{3r}{p}}}{3}$$

The lower value corresponds the the maximum U of lower branch, while the upper value corresponds to minimum U of upper branch. However, the upper branch is not well-modeled by the model because U is usually greater than 1. When $\frac{r}{p} > \frac{1}{3}$, U never jumps to a different branch. When r = 0 (i.e. frictionless case) there is an abrupt transition at $U = \frac{1}{3}$.

3.1 Comparison of simple model and full model

Figure (4) compares the u fields from the full model and the simple model when there is no forcing. The computer model does not exactly match the simple analytical model because it does not conserve angular momentum. The flux of momentum from the lower layer decreases the angular momentum in the computer model. Note that this steady state was generated with 200 v grid points, while we searched for bifurcations using a grid of 50 v points.

4 Results

For a given set of parameters, I ran the model until it came to a steady state (the change in u from one time step to the next was less that some value). I started the run with one value of the forcing at the equator, F_0 , and then used that final state as the initial conditions for the next run, which had a slightly higher forcing. F_0 generally ranged from 0 to 2×10^{-6} ms⁻² in steps of 10^{-8} ms⁻². I ran the model again for the same forcings, this time starting at the highest forcing and decreasing the forcing each run. In this way, I was able to find multiple steady states for some ranges of forcings and parameters; however, this method can not find unstable equilibrium points.

Although the simple model does not depend on the shape of the forcing, the shape of the forcing affects the full model's behavior. The closeness of the full model to the analytical approximation depends on how well angular momentum is conserved by the full model near the equator. When forcing is only at the equator, it increases the wind at the equatorial grid point but has only indirect effects on the surrounding points. Thus, the winds immediately next to the equatorial point are less than the wind at the equator, and the approximation

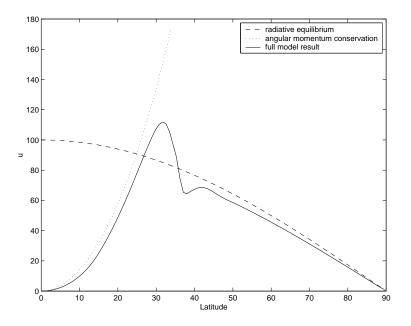


Figure 4: Comparison of zonal momentum from the simple model and the full model with no forcing. The solid line is the computational model result. The dotted line is u from momentum conservation, and the dashed line is the radiative equilibrium result.

of angular momentum conservation starting from the equator is not valid. I could not find any bifurcations when forcing the system only at the equator.

However, once the forcing is spread out a bit, the tropics are closer to angular momentum conservation, and I was able to find multiple equilibria. In each run where I encountered multiple equilibria for some magnitude of the forcin, there were four regions of different behavior:

- 1. For small forcing, the system approximately agrees with the simple analytical model. The only stable solution is a Hadley-cell-like circulation with a small zonal velocity at the equator. The frictional term in the u momentum equation at the equator is much less than the height relaxation term, which increases with increasing F. The dashed lines in Figures 5 through 7 show an example of the steady solution in this region.
- 2. For slightly higher forcing, the system has two steady solutions. One approximates the expected Hadley cell circulation, while the other has a higher u and h. In the lower branch, relaxation back to equilibrium always dominates friction in the u momentum equation at the equator, while in the upper branch, the two are the same order of magnitude. As F increases along the lower branch, the relaxation term increases; however, on the upper branch, it decreases. The dash-dot lines in Figures 5 through 7 show an example of the steady lower branch solution while the dotted lines in Figures 5 through 7 show an example of the steady upper branch solution in this region.
- 3. When the forcing is further increased, the system has only one steady state. u is generally above u_{0eq} , but h is always below h_{eq} . The relaxation term always decreases

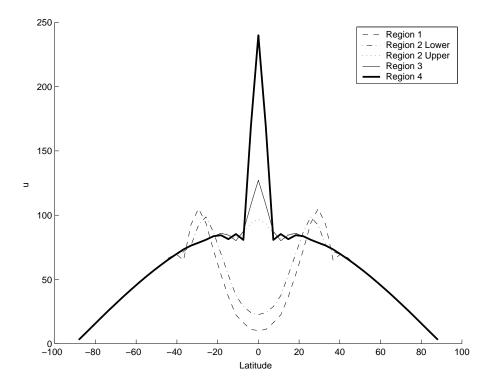


Figure 5: Steady state zonal velocity for $F_0 = 5 \times 10^{-7}$ (dashed), 8×10^{-7} lower branch (dash dot), 8×10^{-7} upper branch (dotted), 8.5×10^{-7} (thin), 12×10^{-7} (thick) for run 1.

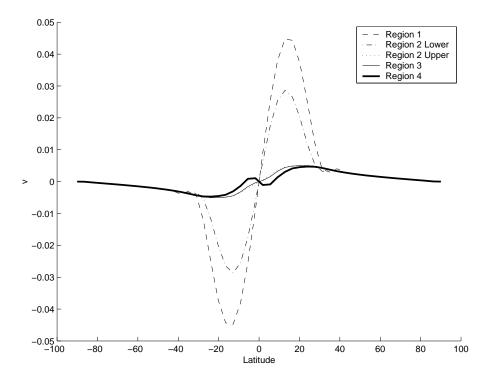


Figure 6: Steady state meridional velocity for $F_0 = 5 \times 10^{-7}$ (dashed), 8×10^{-7} lower branch (dash dot), 8×10^{-7} upper branch (dotted), 8.5×10^{-7} (thin), 12×10^{-7} (thick) for run 1.

with increasing F, so the frictional term dominates by the high end of the region. The thin solid lines in Figures 5 through 7 show an example of the steady solution in this region.

4. For the highest values of the forcing, h_0 is above h_{0eq} . Thus the only term in the equatorial zonal momentum equation which can balance the forcing term is the friction term, and u_0 has only one possible value:

$$u_0 = \frac{F}{k}.$$

The thick solid lines in Figures 5 through 7 show an example of the steady solution in this region.

The size and location of the regions varied from run to run. The base run, run 1, used the values given in section 2, n = 30, and 50 v grid points. Table 1 describes how the other runs differed from run 1 and the ranges of the various regions. Table 2 describes the nondimensional parameters for each run and compares the predicted critical u, u_c on the lower branch to the result obtained in the full model. As expected, c_r was less than predicted in all cases, since the model was not run at exactly the critical forcing magnitude.

Figures 8 through 10 show the values of u and h for the different values of the forcing. The top figure shows how U changes with the forcing. The middle figure shows how 1 - H changes. In the bottom figure, the steady states for the different values of forcing are

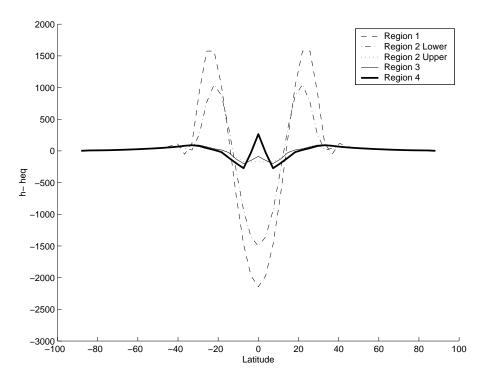


Figure 7: Steady state difference between layer height and relaxation height for $F_0 = 5 \times 10^{-7}$ (dashed), 8×10^{-7} lower branch (dash dot), 8×10^{-7} upper branch (dotted), 8.5×10^{-7} (thin), 12×10^{-7} (thick) for run 1.

plotted along with the lines predicted by the simple model. The solid line corresponds to equation (13). Points for which the simple analytic model of the Hadley cell is a good approximation of the full model lie along this line. As F_0 is changed in a run, the line for equation (14) moves up and down. Where the two lines intersect, we expect a steady state. The dotted line corresponds to equation (14) for the maximum predicted multiple equilibria F_0 , and the dashed line corresponds to the minimum predicted multiple equilibria F_0 .

For the first three runs, $q = 9000 * F_0$, p = 0.0500, r = 0.0045. From the simple model, we expect multiple equilibria in the range $F_0 = 4.9 \times 10^{-7}$ to 10.0×10^{-7} . (In addition, the simple model has three valid solutions for the range $F_0 = 4.9 \times 10^{-7}$ to 5.0×10^{-7} .) These three runs all have multiple steady states for some portion of the range expected by the simple model. One run has multiple steady states for a slightly higher value than expected.

The first three runs study the effect of the shape of F on the full model. The location of the multiple steady equilibria region seems to be within or close to the range predicted by the simple analytical model. However, the range is always less than that predicted by the simple model. The region of multiple equilibria seems to be related to where the model closely conserves angular momentum in the tropics.

Run 4 showed no multiple steady state region, though there is an abrupt transition when $F_0 = 6 \times 10^{-7}$, so that may be some very small region of multiple equilibria at this transition point. For this run, $q = 9000 * F_0$, p = 0.025, and r = 0.0045. Thus, we expect multiple equilibria in the range $F_0 = 4.7 \times 10^{-7}$ to 6.0×10^{-7} . (The simple model has three

Run	Description	1	2	predicted 2	3	4
1	base run	5 - 7.0	7.1-8.4	4.9-10.0	8.5-8.9	9.0-15
2	n=50	3 - 9.5	9.6 - 10.3	4.9 - 10.0	10.4 - 12.3	12.4-20
3	F_2 , n=9	3-8.3	8.4-9.6	4.9 - 10.0	9.7 - 12	?????
4	$\Omega = 14.584 \times 10^{-5},$	1 - 6.0	-	4.7 - 6.0	6.1 - 7.7	7.8 - 10
	$h_{0eq} = 113264$					
5	$h_{0eq} = 113264$	1-6.4	-	4.7 - 6.0	6.5 - 9	10
6	$k = 1 \times 10^{-8}$	1 - 12	-	9.5 - 12.1	13-18	19-20

Table 1: Ranges of F_0 for the different solution regions. The values are in 10^{-7} ms⁻².

Run	p	r	q	predicted u_c	u_c
1	0.05	0.0045	$9000 \times F_0$	0.3819	0.276
2	0.05	0.0045	$9000 \times F_0$	0.3819	0.352
3	0.05	0.0045	$9000 \times F_0$	0.3819	0.306
4	0.025	0.0045	$9000 \times F_0$	0.4406	0.351
5	0.025	0.0045	$9000 \times F_0$	0.4406	0.367
6	0.05	0.009	$9000 \times F_0$	0.4406	0.303

Table 2: Predicted critical u on the lower branch and maximum u obtained on the lower branch of the full model. For cases that do not bifurcate, u_c corresponds to where the height relaxation term transitions from increasing to decreasing with increased forcing.

valid solutions for the range $F_0 = 4.7 \times 10^{-7}$ to 5.0×10^{-7} .) The system transitions to region 3 at the high end of the multiple steady state forcing region.

For Run 4, I increased h_{0eq} along with Ω to prevent the height of the layer from becoming negative. To see the effect of the height alone, Run 5 uses the normal rotation rate but the higher layer height. This run does not even seem to have an abrupt transition; it changes gradually from weakly to strongly superrotating. The values of p, q, and r are the same as for Run 4, since Ω does not affect the simple model (other than determining the critical latitude).

Since friction plays an important role in this system (it affects the locations of the equilibria of the model and becomes important to the behavior of system in regions 3 and 4), I doubled the friction for Run 6. Thus, the parameters for this run are $q = 9000 \times F_0$, p = 0.05, and r = 0.009, and the simple model predicts multiple equilibrium between $F_0 = 9.5 \times 10^{-7}$ and 12.1×10^{-7} , with three valid solutions for the range $F_0 = 9.5 \times 10^{-7}$ to 10.0×10^{-7} . I found no region of multiple equilibria, and the steady state value of u does not show any abrupt changes.

5 Rossby waves

We attempted to add the effects of breaking Rossby waves to the full model. At each time step, Rossby waves with a certain distribution of phase speeds and pseudo-angular-

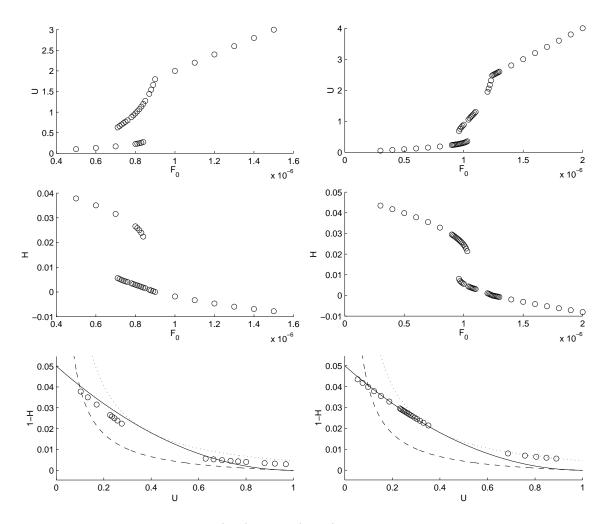


Figure 8: Runs 1 (left) and 2 (right). See text for explanation.

momentum were introduced at a certain latitude. These Rossby waves moved towards the equator (and across to the other hemisphere, if necessary) and "broke" at the first latitude where their angular phase speed was greater than or equal to the angular momentum of the zonal winds. The breaking waves decreased the angular momentum at that latitude and thus reduced the zonal winds.

I used wave speeds, c, distributed between 5 and 45 m/s. The distribution of angular pseudomomentum deposited when waves of a particular speed break, P(c) is

$$P(c) = \frac{P_{max}}{h\Delta\phi\cos\phi} e^{-\left(\frac{c-25}{10}\right)^2}$$

The addition of the waves allows for the possibility of periodic solutions. The waves break at a certain latitude, which slows down the flow there (and through advection, surrounding areas). Thus, the waves start breaking earlier (i.e. further poleward) and decreasing the flow there. The waves continue breaking earlier and earlier until they get to the

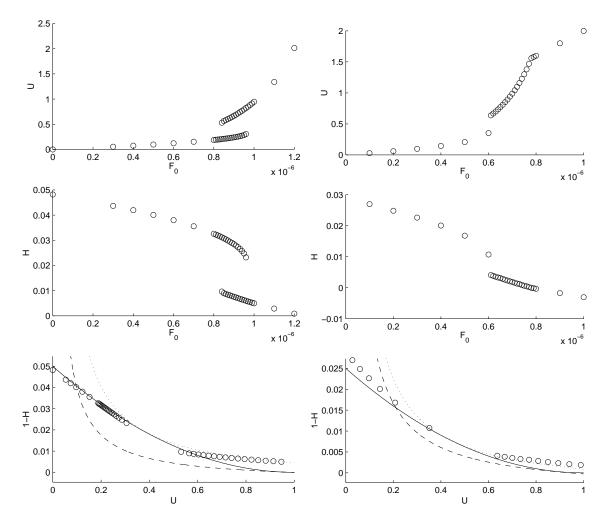


Figure 9: Runs 3 (left) and 4 (right). See text for explanation.

jet. Eventually, the disturbance moves to a region where u is high enough that some of the lower phase speed waves can pass through to the equatorial region. Another disturbance starts before the first one gets to the jet.

I studied the behavior of the waves with no forcing. The system reached a stable periodic solution. However, the period of the solution varied with the grid resolution. Thus, we did not pursue this parameterization further.

6 Conclusion

It is possible to get bifurcations in the superrotation strength in an axisymmetric model for some parameter ranges. When bifurcations exist, the stable equilibria lie along two branches of u values as the forcing is changed. On the lower branch, damping due to height relaxation increases with increasing F; on the upper branch, the damping decreases with increasing F.

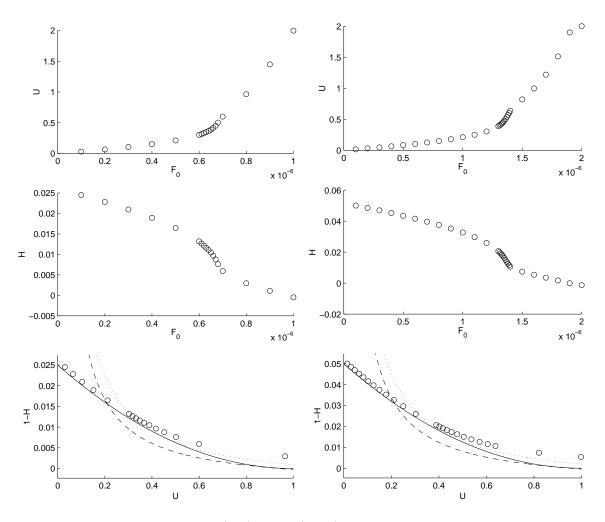


Figure 10: Runs 5 (left) and 6 (right). See text for explanation.

Although the simple model approximately predicts where the full model will have multiple equilibria, the range is smaller than predicted and sometimes multiple equilibria are not present at all. The presence and location of the bifurcation has something to do with how well angular momentum is conserved in tropics, which depends on forcing. However, the exact relationship is not clear.

7 Acknowledgments

I would like to thank my project supervisor, Isaac Held, for his help with all aspects of my project. I would also like to thank Jeff Moehlis for help with the nonlinear dynamics and for his general enthusiasm for the project, which increased my own. Thanks to Giulio for model discussions. Thanks to Cheryl and Tevon for providing the music and everyone who went dancing with me for keeping me sane. Thanks to Chris and his green car for providing the transportation. GFD is fun and easy.

References

- M. J. Suarez and D. G. Duffy, "Terrestrial superrotation: A bifurcation of the general criculation," J. Atmos. Sci. 49, 1541 (1992).
- [2] R. Saravanan, Ph.D. thesis, Princeton University, Princeton, NJ 08544, 1990.
- [3] H.-P. Huang, K. M. Weickmann, and C. J. Hsu, "Trend in atmospheric angular momentum in a transient climate change simulation with greenhouse gas and aerosol forcing," J. Clim., submitted.
- [4] I. M. Held, "Equatorial superrotation in earth-like atmospheric models," Bull. Am. Met. Soc., in preparation.
- [5] I. M. Held and A. Y. Hou, "Nonlinear axially symmetric circulations in a nearly inviscid atmosphere," J. Atmos. Sci. 37, 515 (1980).